



A COMPARATIVE STUDY ON THE SYNTHESIS CHARACTERIZATION OF POLY (DIPHENYL AMINE) AND POLY (DIPHENYL AMINE DOPED ZINC OXIDE) NANO PARTICLES

^{1*}Vetriselvi V, ²Jeevi Esther Rathnakumari R, ³Deva kumar J, ⁴Vanmathi M, ⁵Bessanlin

¹Assistant Professor, ²Head & Associate Professor, ³Assistant Professor, ⁴Student, ⁵Student

^{1,4,5} P.G Department of Chemistry ,Nazareth Margoschis College at Pilliyanmanai, Nazareth, Thoothukudi, Tamilnadu, India.

² Department of Chemistry ,Nazareth Margoschis College at Pilliyanmanai, Nazareth, Thoothukudi, Tamilnadu, India.

³Department of Chemistry, Annai Violet Arts and Science College, Chennai – 600053, Tamilnadu, India.

ABSTRACT: Polymerization of diphenylamine (PDPA) and diphenylamine doped with zinc oxide nanoparticles (PDPA/ZnO) were carried out in a room temperature. The prepared conducting PDPA and PDPA/ZnO were characterized through UV–Visible spectroscopy, Fourier transform infrared spectroscopy, X-ray diffraction, scanning electron microscopy. The charge transitions between benzenoid and quinonoid bands were observed by UV–Vis spectrum analysis. From the FTIR spectroscopy quinonoid and benzenoid rings were identified through vibrational bands between 1594 and 1490 cm^{-1} for both PDPA and PDPA/ZnO. The XRD data shows the crystalline nature increases for PDP/ZnO. The SEM images at different magnification had flakes like arrangement. The presence of zinc was confirmed by the EDX. From the CV studies PDPA and PDP/ZnO exhibit redox properties of PDPA and PDP/ZnO. The DSC shows the T_g was around 54°C.

Index Terms – diphenylamine, zinc oxide, PDPA/ZnO, quinonoid, benzenoid.

I. INTRODUCTION

The emergence of intrinsically conducting polymers (ICP) has constituted a significant milestone in modern analytical science. The typical CPs includes polyaniline, polypyrrole, polythiophene and their derivatives. The most common forms of ICPs in their neutral states are insulators called conjugated polymers. However, these neutral conjugated polymers can be converted into semi-conductive or conductive states through chemical or electrochemical redox reactions. Intrinsically conducting polymers or electro active conjugated polymers exhibit interesting electrical and optical properties previously found only in inorganic systems. A key requirement for a polymer to become intrinsically electrically conducting is that there should be an overlap of molecular orbitals to allow the formation of delocalized molecular wave function. Besides this, molecular orbitals must be partially filled so that there is a free movement of electrons throughout the lattice can occur (Xu, Peng, et al.2006). To extend the functions or to improve the performances of these polymers, ICPs are frequently doped with other functional materials to form composites. Due to their unique conductive properties, they are usually employed in significant applications in chemistry, physics, electronics, optics, materials and biomedical science which have prompted the need for analytical methodologies to characterize and to control the quality of these materials (Jang, Jyongsik. 2006). Intrinsically conducting polymers (ICPs) applications in a wide variety of advanced technical and biotechnical devices has prompted intensive research in their opto-electronic, electro-optical, chemical, electrochemical, organic light emitting diodes (OLED), solar photovoltaic (solar cells), rechargeable batteries, fuel cells, sensors, actuators, protective coatings, catalysis, tissue engineering, drug-delivery systems (Zhang, Haiqiu, et al. 2008). Conventional polymers usually serve as the matrix, which result in a special class of hybrid materials termed “polymeric nanocomposites”. This composite material differs from the pure polymer with respect to some of the physical and chemical properties and hence it is useful for many applications in different field (Pfaendner, Rudolf.2010). Nanocomposites containing nanosized metal oxides have been extensively studied since they exhibit interesting properties with many applications such as quantum electronic devices, magnetic recording materials, sensors, capacitors, smart windows, toners in photocopying, conducting paints, and rechargeable batteries.

II. RESEARCH METHODOLOGY

2.1. Synthesis of Poly Diphenyl Amine (PDPA)

Poly Diphenyl Amine (PDPA) was synthesized through oxidative polymerization reaction. Monomers of Diphenyl Amine (PDPA) 0.1M were dissolved in 100 ml of a 0.1M HCl. Ammonium persulphate 0.1M dissolved in 100 ml of a 0.1 M HCl solution was added drop wise and stirred continuously for 48 hours to complete the reaction. The resulting product was thoroughly washed

with de-ionized water until the solution turned colorless. The product was dried in a vacuum oven at 50°C for 24 h (H.Yuvaraj et al. 2014).

2.2. Synthesis of Poly Diphenyl Amine /ZnO Nanocomposites

Poly Diphenyl Amine/ZnO Nanocomposite were synthesized through oxidative polymerization. Diphenyl Amine (0.1M), was dissolved in 100 ml of a 0.1M HCl. ZnO nanoparticles (10% wt/wt based on the co-monomer content) were then dispersed in the solution by intense stirring for 30 min. Finally, Ammonium per sulphate (0.1M) dissolved in 100 ml of a 0.1M HCl solution was added drop wise and stirred continuously for 48 hours to complete the reaction. The resulting product was thoroughly washed with de-ionized water until the solution turned colorless. The product was dried in a vacuum oven at 50°C for 24 h. The nanocomposite containing 10% ZnO was chosen for this study because of its higher conductivity than the 5% nanocomposite (F. L. Deepak. et al 2005).

2.3. Experimental Techniques

The NIR - UV - Visible spectra of the synthesized conducting polymer and its nano composite were recorded using a UV-Vis spectrophotometer, VARIAN CARRY 5000, at the range of 200nm to 2000 nm. FTIR spectra were recorded by Jasco FT-IR - 4600 TYPE A. Fourier Transform Infrared spectrometer in the wave number range of (400- 4000 cm^{-1}). The XRD studies synthesized polymer are characterized by BRUKER AXS. The diffraction system based with Cu tube anode with voltage 40kV, current 35mA & wave length $\alpha 1 K = 1.5418 \text{ \AA}$. The start angle (2θ) was 5° and the end angle was 80°. Bragg's Law ($n\lambda = 2d \sin\theta$) was used to compute the crystallographic spacing. The scanning electron microscope images were recorded using JEOL JSM 5600 LV SEM and magnification rate of 1500 to 15000 units at 20 KeV. The Cyclic voltammetry studies was carried out using BIO-LOGIC SAS SP-150 at the scan rate of $dE/dT=20.0 \text{ mV/s}$ and $E_{\text{Range}} = -2.5 \text{ to } 2.5\text{V}$. In the present study, the DSC studies were carried using METTLER TOLEDO with the heating rate of $10^\circ\text{C min}^{-1}$ in the temperature range $30^\circ - 400^\circ\text{C}$ under nitrogen atmosphere.

III RESULTS AND DISCUSSION

3.1 NIR-UV Visible spectra of PDPA and PDPA/ZnO

The UV-vis spectrum of the Poly Diphenyl Amine (PDPA) and Poly Diphenyl Amine doped Zinc oxide nanocomposites PDPA/ZnO are shown in Fig.1(a) the uv-visible spectra of PDPA and PDPA/ZnO peaks at 303 nm and 313 nm shows $\pi \rightarrow \pi^*$ transition for both PDPA and PDPA/ZnO; 370, 354 are attributed to polaron band $\rightarrow \pi^*$ transition and the π to the localized polaron band of doped poly diphenyl amine in its emeraldine salt form, respectively (Kuppusamy, et al. 2013). The transition of charge carriers is analyzed in benzenoid structure and quinonoid ring of the prepared conducting polydiphenylamine using UV-visible spectrum. The characteristics absorption of a conducting polyaniline and derivatives of polyaniline i.e.poly diphenylamine plays a vital role in the utilization of the materials in the optoelectronic applications. From the fig.1(a) the peak in wavelength range 303 nm is due to the $\pi-\pi^*$ transition of benzenoid ring, the peak in wavelength range 420 nm is due to polaron - π^* transition and the peak in wavelength range 830 nm is due to π - polaron transition. The Fig. 1(a) demonstrates UV-visible absorption spectrum of PDPA/ZnO nano composite. The two major absorption peaks and one at less absorption peak are observed at 313 nm and 620 nm and 834 nm. The peak 313 nm is due to the $\pi-\pi^*$ transition which is related to the extent of conjugation between the adjacent phenylene rings in the polymeric chain and the peak at 620 nm is owing to the shifting of electron from benzenoid ring to quinonoid ring and the peak at 834 nm is caused by π - polaron transition. These peaks have been assigned to transition from valance band to conduction band at 320 nm and charge transfer between benzenoid and quinonoid rings due to free nonbonding electrons that can absorb relatively low energy radiation and these are well agreed with the results of Jing et al. 2005 & Yang et al.2008).

3.2 FT-IR Spectra of Poly Diphenyl Amine

The FT-IR spectra of PDPA shown in the fig.1(b). The major IR absorption bands at 1594 and 1415 cm^{-1} are the characteristic bands due to quinonoid-benzenoid rings, the peak at 3822 cm^{-1} is for N-H bond (Boyer, M. I., et al.2000). The other IR characteristics are absorption peaks at 1153, 1079 and 988 cm^{-1} . The peaks at 1594 and 1490 cm^{-1} are assigned to the C- C stretching of quinonoid rings and benzenoid rings respectively. The peak at 1314 cm^{-1} corresponds to stretching of C-N. The peaks at 1153 and 874 cm^{-1} are attributed to the aromatic C-H in-plane bending and out-of-plane deformation of C-H in the substituted benzene ring (Marcelo M., et al. 2013).

The FT-IR PDPA/ZnO is shown in the Fig. 1(b). The major IR absorption bands at 1589 and 1474 cm^{-1} are the characteristic bands due to quinonoid-benzenoid rings, the band at 1317 cm^{-1} is for N-H bond. The other IR characteristics are absorption peaks at 1085, 1024 and 993 cm^{-1} . The band at 3375 cm^{-1} for N-H bond. The band peaks at 1085 and 1024 cm^{-1} are attributed to the aromatic C-H in-plane bending and out-of-plane deformation of C-H in the substituted benzene ring (Sundaraganesan, B. N., et al. 2005).

3.3 XRD spectra of PDPA and PDPA/ZnO

Figure 1(c) shows the X-ray diffraction spectrum (XRD) patterns of PDPA and PDPA/ZnO nanocomposites and their values are given in the table 1. PDPA has X-ray diffraction pattern consisting of five peaks at with maximum intensity at 2θ : 9, 20, 25, 28, and 37 has a similar profile as reported in the literature for polyaniline. The peak at 25 can be assigned to the scattering from polyaniline chains at interplanar spacings (Zhang Xiao-Gang et al. 2005). PDPA/ZnO nanostructure from interfacial polymerization also has the main peaks approximately at 15 and 25 values of 2θ . From the result, we can draw conclusion that this sample is crystalline material as well. It has been reported that the ratio of half-width to height (HW/H) of an X-ray diffraction peak reflects the order of the polymer crystallinity. The crystallinity and orientation of conducting polymers have been of much interest, because more highly ordered systems can display a metallic conductive state and may influence the anticorrosion performance. However, the diffractive peaks of poly diphenyl amine obtained using conventional polymerization have become weak, which indicates that the degree of crystallinity is decreased (Epstein. et al. 2005). The peaks with maximum intensity at 9, 20, 25, and 28 of 2θ were repeated in the PDPA/ZnO and the other peaks at 14, 18, 21, and 32 are due to the influence of the zinc oxide nano composites. This confirms that the zinc oxide nano composites are incorporated into the polymeric back bone of PDPA. PDPA was found to be semicrystalline in nature while on doping with ZnO the crystallinity further increases leading to maximum number of crystalline peaks in the X ray diffraction pattern (Kuppusamy, et al. 2013).

TABLE 1 XRD data for PDPA and PDPA/ZnO

PDPA					PDPA/ZnO				
Pos. (°2θ)	Ht. (counts)	d-spacing (Å)	Relative intensity (%)	Crystalline size (nm)	Pos. (°2θ)	Ht. (counts)	d-spacing (Å)	Relative intensity (%)	Crystalline size (nm)
9.307	2460	9.49477	31.4	0.105	9.399	9528	9.40153	73.4	0.106
20.038	7842	4.4277	100	0.226	14.044	945	6.30092	7.3	0.159
25.224	6151	3.52782	78.4	0.284	18.717	7696	4.73706	59.3	0.211
27.814	5339	3.20494	68.1	0.312	20.226	12130	4.38687	93.4	0.228
37.328	1038	2.40703	13.2	0.415	21.618	12985	4.10746	100	0.244
					25.225	4107	3.52766	31.6	0.283
					28.529	3057	3.1262	23.5	0.320
					32.503	1141	2.75252	8.8	0.363

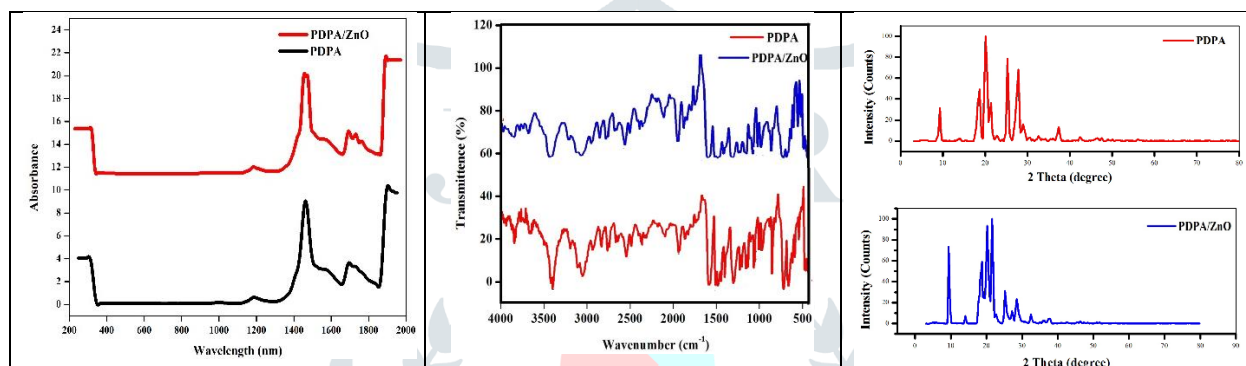


Figure 1. (a) UV-Vis of PDPA and PDPA/ZnO. (b) FT-IR of PDPA and PDPA/ZnO. (c) XRD of PDPA and PDPA/ZnO.

3.4 Electrochemical behaviour of PDPA and PDPA/ZnO using ethanol and sulphuric acid

The electrochemical behaviour of the synthesized PDPA and PDPA/ZnO were carried out using cyclic voltammetry studies using ethanol as a solvent. the CV studies for PDPA and PDPA/ZnO are given in the fig.4 (a) & (b) shows both the anodic and cathodic peak potential. From the fig.2(a) the cathodic peak potential and the peak current were found to be $E_{pc} = 0.4972$ V, $I_{pc} = 4.428 \times 10^{-3}$ mA. The anodic peak potential and the peak current were found to be $E_{pa} = -0.5252$ V, $I_{pa} = -1.941 \times 10^{-2}$ mA (Muthusankar, E., et al. 2020). From the fig. 2(b) PDPA/ZnO has the cathodic peak potential and the peak current at $E_{pc} = 0.5003$ V, $I_{pc} = 4.43 \times 10^{-3}$ mA. The anodic peak potential and the peak current were found to be $E_{pa} = -0.4996$ V, $I_{pa} = -1.742 \times 10^{-2}$ mA. The ΔE_p value was found to be -1.0224 for PDPA and be -0.9999 for PDPA/ZnO in ethanol (Muthusankar, E., et al. 2019).

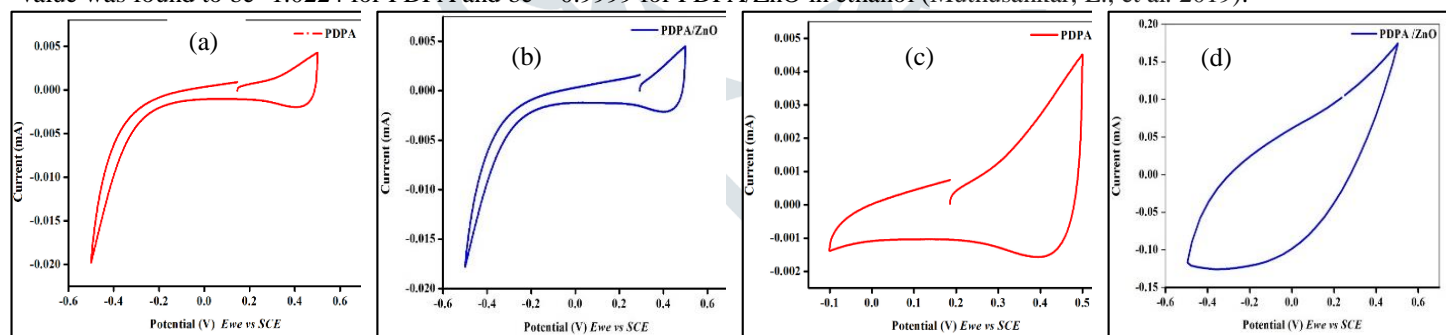


Figure 2 Cyclic Voltammetric response of the (a)PDPA and (b)PDPA/ZnO hybrid modified electrode in ethanol (c)PDPA and (d)PDPA/ZnO hybrid modified electrode in 0.1 M solution of Sulphuric acid at the scan rate of 20.0 mV/s

The electrochemical studies of PDPA and PDPA/ZnO exhibits two redox processes. The first oxidation peak for PDPA appears at 0.456V for the cathodic potential during the cathodic scan and the anodic potential appears at -0.4886 V during the anodic scan. The oxidation peak at 0.456V is due to the removal of one electron from the amino group to form a positively charged N, N'- diphenylbenzidine type ion radical ($DPA^+ \bullet$). Then, a removal proton from two such monomer radicals dimerizes to form a dimer of DPA. The coupling takes place at the para position. Further oxidation leads to the growth of PDPA chain. During negative scan, the polymer is reduced by the protonation of the nitrogen atom in the backbone of the polymer. The reduction peaks appear at -0.4886 V during the cathodic scan (Alvi, Farah, et al. 2010). The same trend was observed in the case of PDPA/ZnO but both the oxidation and the reduction peak potential and varies due to the doping of the ZnO composites. 1.1586×10^{-1} mA. The figure 3.12 PDPA has the cathodic peak potential $E_{pc} = 0.4949$ V and the peak current were found to be, $I_{pc} = 1.732 \times 10^{-1}$ mA. The anodic peak potential $E_{pa} = -0.4931$ V and the peak current were found to be, $I_{pa} = -0.1196$ mA. The anodic peak potential appears -0.1156 V and -0.1183×10^{-1} mA is due to the coupling of the two anodic peaks (Zhang, Haiqiu, et al. 2008). The ΔE_p value was found to be -0.9446 for PDPA and be -0.9880 for PDPA/ZnO.

3.5. Surface morphological study of polymer by SEM of PDPA and PDPA/ZnO

The SEM images of PDPA are shown in the Fig. 3 at different magnification. PDPA appears as solid polymeric irregular rigid flakes like arrangement (Lim, H et al. 2009). The SEM images of PDPA /ZnO are shown in the fig.2 at different magnification. The doped zinc oxide nano composites appear as shiny spherical crystals which were incorporated on to the polymeric matrix. The doped polymers of zinc oxide PDPA/ZnO nano composites have the better efficiency when compared to the polymer PDPA/ZnO. The SEM image of PDPA/ZnO nanoparticles at X 10,000 magnification shows ZnO particles are spherical in shape with smooth surface and the size of the particles around 132 nm (Alwan,et al 2015).

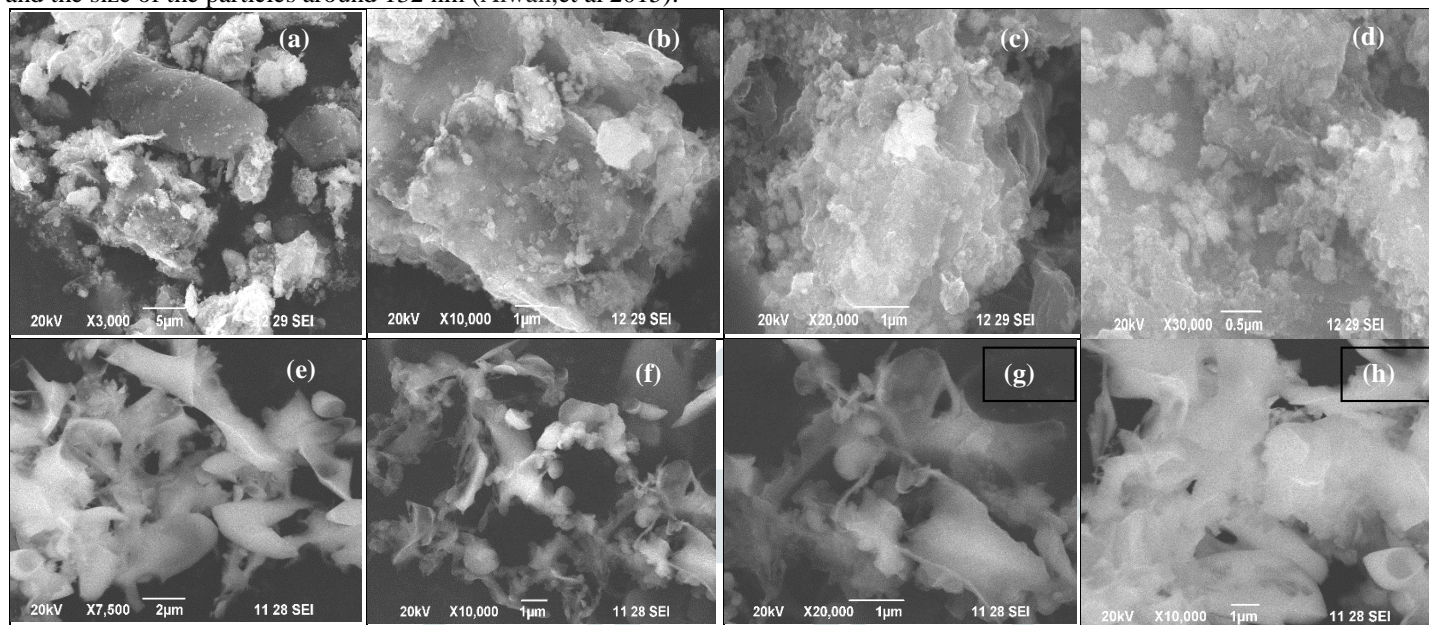


Figure 3. Comparison of SEM images of PDPA (a), (b), (c), (d), and PDPA/ZnO (e), (f), (g) at different magnification

3.6. Energy Dispersive X-ray diffraction spectroscopy (EDX)

Figure 4(a) shows the EDX spectrum of PDPA with the absence Zn, but in fig.3(b) for PDPA/ZnO nanoparticles has Zinc. The strong peaks observed in the spectrum related to carbon, oxygen and zinc. Carbon present in the polymer was observed in the EDS. The elemental constitution of ZnO nanoparticles with three major peaks were at 1.2 keV, 8.6 keV and 9.6 keV (Raj et al. 2016). Again the graph shows the presence of Si. This is due to the substrate over which it was held to do the SEM characterization.

3.7 DSC of PDPA and PDPA/ZnO

The different phase temperature was observed from DSC curve and the glass transition temperature (T_g). The DSC of PDPA and PDPA/ZnO is given in the fig. 5. The T_g value of PDPA was found to be 55.03 °C and T_c was found to be 285.41°C for PDPA. The T_g = 54.93 °C and T_c was found to be 282.29 °C for PDPA/ZnO. As the crystallinity nature of PDPA/ZnO increases the crystalline temperature T_c decreases when compared to the pure PDPA. The crystalline nature was further confirmed by the XRD studies of both PDPA and PDPA/ZnO.

For the polymer PDPA and PDPA/ZnO, two exotherms were noticed in the DSC curves fig.5 in comparison with the both exotherms the first exotherm observed around 55.03 °C was attributed to the T_g value represents the decomposition of PDPA content in the polymer. This exotherm showed a shift to a higher temperature region of 285.41°C corresponds to the T_c in comparison with the decomposition of PDPA/ZnO on increasing the ZnO. The PDPA/ZnO has less T_c value due to its crystallinity nature (Ozkan, S. Zh, et al. 2015).

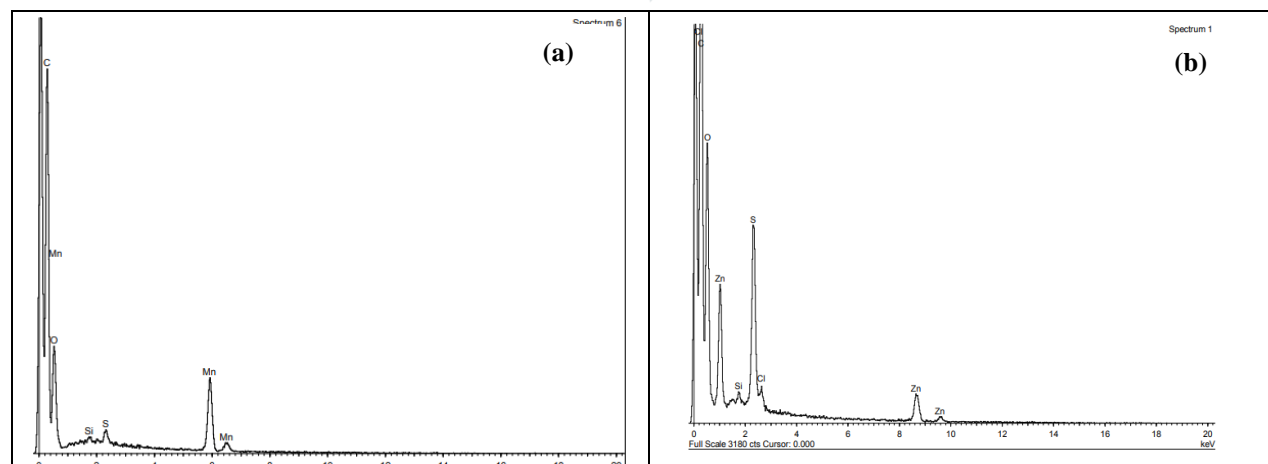


Figure 4. EDX spectrum of (a)PDPA and (b) PDPA/ZnO nanoparticles

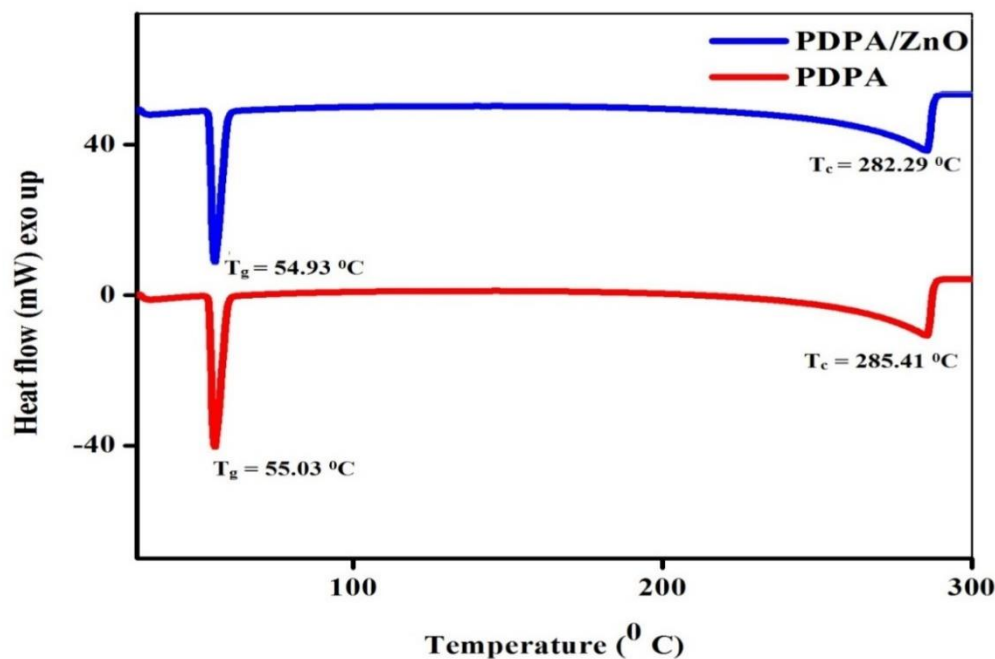


Figure 5. DSC of PDPA and PDPA/ZnO

IV. CONCLUSION

The present research work comprises of the synthesis and characterization of Poly Diphenylamine (PDPA) and its zinc oxide nano composites PDPA/ZnO. PDPA and PDPA/ZnO were synthesized by chemical oxidative polymerization. The NIR-UV visible spectra reveal the presence of both benzenoid and quinonoid transitions responsible for conducting polymers. The FT-IR spectra confirms the presence of secondary -NH stretching and the other bands corresponds to the synthesized PDPA and PDPA/ZnO. The XRD data substantiate the semicrystalline nature of both PDPA and PDPA/ZnO. The crystalline size was calculated using the Debye - Scherrer formula. The SEM images of both PDPA and PDPA/ZnO were investigated. The PDPA/ZnO were in spherical shape in nano scale further confirms the doping of the ZnO nano particles into polymeric chain. The SEM-EDS shows the presence of Zn peak authenticate the formation of PDPA/ZnO nano composites. The electrochemical studies of the synthesized PDPA and PDPA/ZnO were carried out using cyclic voltammetry by using ethanol and 0.1 M of sulphuric acid. Better response attained using 0.1 M of sulphuric acid. Both the oxidation and the reduction peak potentials and current were obtained indicated the redox reaction had taken place.

V. ACKNOWLEDGEMENT

The authors acknowledge the instrument facilities provided by the SAIF, IIT-Madras and NRC, SRMIST Chennai, STC- Cochin.

References

- [1]. Abdiryim, Tursun, Zhang Xiao-Gang et al. , and Ruxangul Jamal. 2005. "Comparative studies of solid-state synthesized polyaniline doped with inorganic acids." *Materials Chemistry and Physics* 90.2-3: 367-372.
- [2]. Alwan, R.M., Kadhim, Q.A., Sahan, K.M., Ali, R.A., Mahdi, R.J., Kassim, N.A. and Jassim, A.N., 2015. Synthesis of zinc oxide nanoparticles via sol-gel route and their characterization. *Nanoscience and Nanotechnology*, 5(1), pp.1-6.
- [3]. Boyer, M. I., et al. 2000 "Vibrational study of the FeCl₃-doped dimer of polyaniline; a good model compound of emeraldine salt." *The Journal of Physical Chemistry B* 104.38: 8952-8961.
- [4]. Alvi, Farah, et al. 2010 "Evaluating the chemio-physio properties of novel zinc oxide-polyaniline nanocomposite polymer films." *Polymer journal* 42.12 : 935-940.
- [5]. Chiou NR, Epstein AJ 2005. Polyaniline nanofibers prepared by dilute polymerization. *Adv Mater* 17:1679–1683.
- [6]. Epstein. et al. 2005. "Polyaniline nanofibers prepared by dilute polymerization." *Advanced Materials* 17.13: 1679-1683.
- [7]. F. L. Deepak. et al. 2005. "Tuning the bandgap of ZnO by substitution with Mn²⁺, Co²⁺ and Ni²⁺." *Solid State Communications* 135.6: 345-347.
- [8]. Gopalakrishnan, Kuppusamy, et al. 2013 "Catalytic-assisted synthesis, characterization and low frequency AC conduction of nanostructured conducting polyaniline." *Iranian Polymer Journal* 22: 43-52.
- [9]. Haldorai, Yuvaraj et al. 2014. "ZnO nanoparticles dispersed poly (aniline-co-o-anthranilic acid) composites: Photocatalytic reduction of Cr (VI) and Ni (II)." *Polymer composites* 35.5: 839-846.
- [10]. Jang, Jyongsik. 2006. "Conducting polymer nanomaterials and their applications." *Emissive materials nanomaterials* : 189-260.
- [11]. Jing, X., Wang, Y., Wu, D. and Qiang, J., 2007. Sonochemical synthesis of polyaniline nanofibers. *Ultrasonics Sonochemistry*, 14(1), pp.75-80.
- [12]. Lim, H., Kassim, A., Huang, N., Khiewc, P. and Chiu, W., 2009. Three-dimensional flower-like brushite crystals prepared from high internal phase emulsion for drug delivery application. *Colloids and Surfaces A: Physicochemical and Engineering Aspects*, 345(1), pp.211-218.

- [13]. Muthusankar, E., et al. 2020. "Fabrication of amperometric sensor for glucose detection based on phosphotungstic acid–assisted PDPA/ZnO nanohybrid composite." *Ionics* 26 : 6341-6349.
- [14]. Muthusankar, E., Vinoth Kumar Ponnusamy, and D. Ragupathy. 2019. "Electrochemically sandwiched poly (diphenylamine)/phosphotungstic acid/graphene nanohybrid as highly sensitive and selective urea biosensor." *Synthetic Metals* 254 : 134-140.
- [15]. Nobrega, Marcelo M., et al. 2013 "Emeraldine salt form of polyaniline as a probe molecule for surface enhanced Raman scattering substrates excited at 1064 nm." *The Journal of Physical Chemistry C* 117.35: 18199-18205.
- [16]. Ozkan, S. Zh, et al. 2015 "A magnetic metal/polymer nanocomposite material based on poly (diphenylamine) and Fe₃O₄ nanoparticles." *Russian Chemical Bulletin* 64 : 196-201.
- [17]. Pfaendner, Rudolf. 2010. "Nanocomposites: Industrial opportunity or challenge?." *Polymer Degradation and Stability* 95.3 : 369-373.
- [18]. Sundaraganesan, B. N., et al. 2005 "FT-Raman and FT-IR spectra, vibrational assignments and density functional studies of 5-bromo-2-nitropyridine." *Spectrochimica Acta Part A: Molecular and Biomolecular Spectroscopy* 61.13-14 : 2995-3001.
- [19]. Venkatachari. G et al. 2006 "Synthesis and anticorrosion properties of polydiphenylamine blended vinyl coatings." *Synthetic metals* 156.18-20 : 1208-1212.
- [20]. Xu, Peng, et al. 2006 "Synthesis of TiO₂–SiO₂/polymer core–shell microspheres with a microphase-inversion method." *Journal of Polymer Science Part A: Polymer Chemistry* 44.12: 3911-3920.
- [21]. Yang J, Ding Y, Zhang J 2008. Uniform rice-like nanostructured polyanilines with highly crystallinity prepared in dodecylbenzene sulfonic acid micelles. *Mater Chem Phys* 112:322–324.
- [22]. Zhang, Haiqiu, et al. 2008 "Composite membranes based on highly sulfonated PEEK and PBI: Morphology characteristics and performance." *Journal of Membrane Science* 308.1-2: 66-74.
- [23]. Zhao, Yu, et al. 2016 "ZnO-nanorods/graphene heterostructure: a direct electron transfer glucose biosensor." *Scientific reports* 6.1: 32327.

